FUSION TECHNOLOGY

Annual Report of the Association EURATOM/CEA 2003

(full report)

Compiled by : Ph. MAGAUD and F. Le VAGUERES

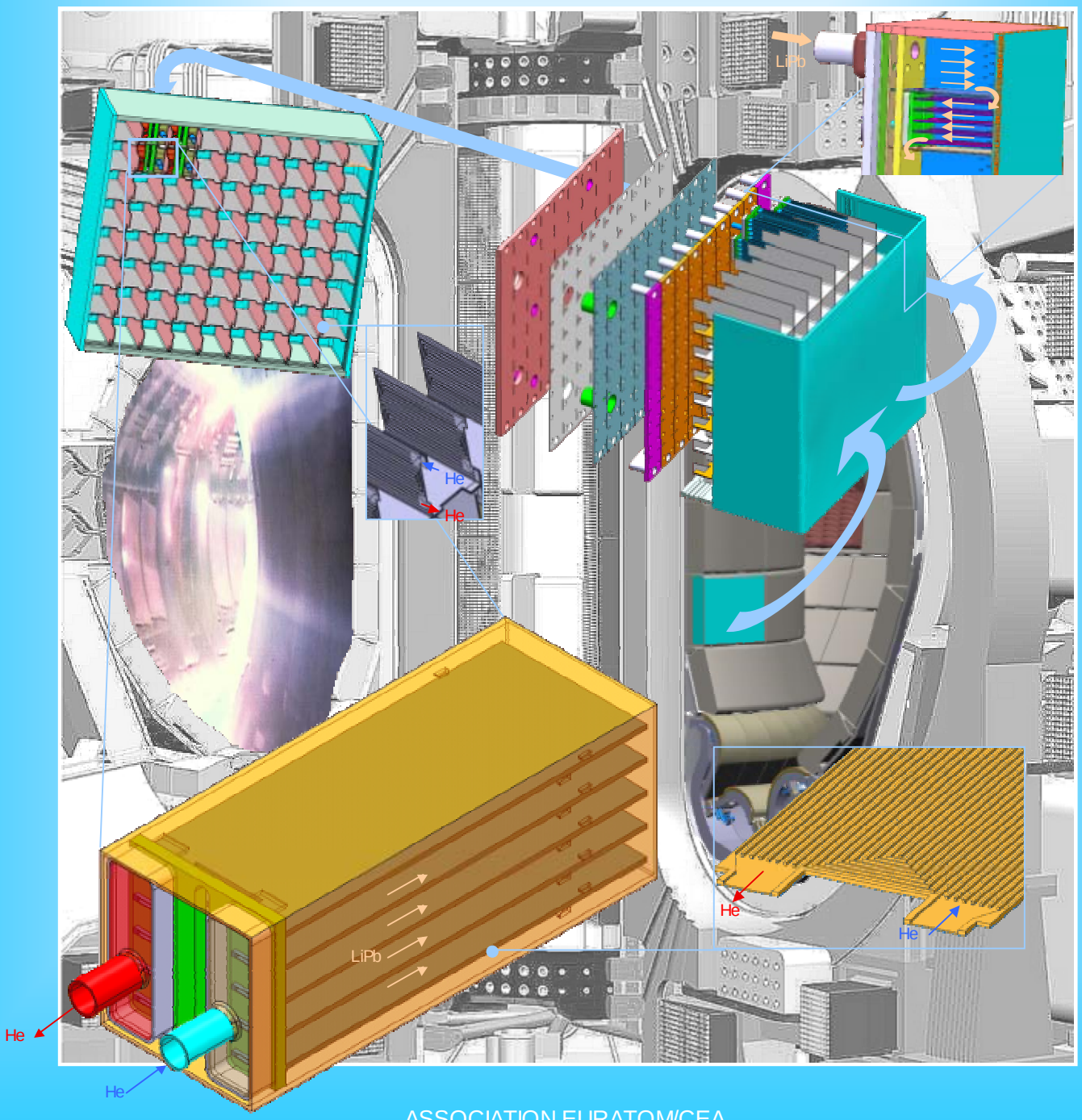

ASSOCIATION EURATOM/CEA
DSM/DRFC
CEA/CADARACHE
13108 Saint-Paul-Lez-Durance (France)

FUSION TECHNOLOGY

Annual Report of the Association CEA/EURATOM

2003

(full report)

Compiled by : Ph. MAGAUD and F. LE VAGUERES

ASSOCIATION CEA/EURATOM
DSM/DRFC
CEA CADARACHE
13108 Saint-Paul-Lez-Durance (France)

Tél. : 33 - 4 42 25 46 59
Fax : 33 - 4 42 25 64 21
e-mail : dirdrfc@drfc.cad.cea.fr
Web : http://www-fusion-magnetique.cea.fr

This report is also available on-line at : http://www-fusion-magnetique.cea.fr

Cover : *Exploded view of the Helium Cooled Lithium Lead (HCLL) breeding blanket concept.*

CONTENTS

Plasma Facing Components

Remote Handling

Magnet Structure

Tritium Breeding and Materials

Breeding Blanket

Water Cooled Lithium Lead (WCLL) blanket

Helium Cooled Pebble Bed (HCPB) blanket

Helium Cooled Lithium Lead (HCLL) blanket

Structural materials development

Reduced Activation Ferritic Martensitic (RAFM) steels

Advanced materials

Neutron source

Safety and Environment

System Studies

Power Plant Conceptual Studies (PPCS)

Socio-economics studies

ITER Site Preparation

Design Support and Procurement

JET Technology

Physics Integration

Heating Systems

Diagnostics

Tritium Breeding and Materials

Breeding Blanket

Materials Development

Structural Materials

Safety and Environment

EUROPEAN FUSION DEVELOPMENT AGREEMENT TECHNOLOGY PROGRAMME

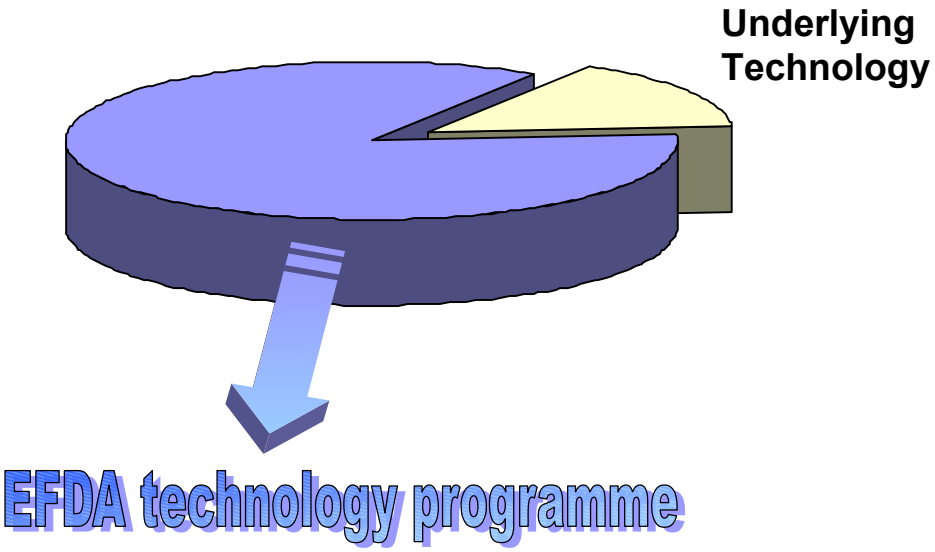

*European ITER Site Study tasks excluded

TW1-TSS-SEA3.5

Task Title: IN VESSEL HYDROGEN DEFLAGRATION/DETONATION ANALYSIS

INTRODUCTION

The hydrogen sources in the vacuum vessel (VV) of ITER are the following:

- Chemical reaction between beryllium and steam.
- H_2 inventory of the cryopumps.
- H_2 released in the cooling loops.
- Co-deposited layers.
- H_2 inventory in the VV during plasma operation.

The hydrogen sources which are currently present in the VV are listed in the following table:

Type	VV inventory [mole]
3 HNBI / 1 DNBI (Neutral Beam Injector cryopumps)	100
Torus cryopumps	40
H_2 in 3 FW cooling loops	440
H_2 in DV cooling loop	180
Nominal H_2 in VV during plasma operation (D/T)	0.2

Some accidental scenarios lead to the simultaneous presence of hydrogen and air inside the vacuum vessel. The sources of hydrogen are those mentioned in the previous section. The air release into the VV can come from a Loss of Vacuum Accident (LOVA) or from a double Loss of Coolant Accident (ex-vessel + induced in-vessel LOCA resulting in the bypass of the first barrier).

2003 ACTIVITIES

Two kinds of scenarios, involving small quantities of hydrogen, have been identified for the reference events in ITER.

- The loss of vacuum through one VV/cryostat penetration line (dry scenario): in this case, the hydrogen released into the vacuum vessel comes from the cryopumps of the Heating Neutral Beams and the Diagnostic neutral Beam modules.

- The large Divertor ex-vessel coolant pipe break (wet scenario): in this case, the hydrogen comes from the chemical reaction between the steam and the protective materials of the Plasma Facing components.

A complementary analysis of the dry scenario has been done using simplified hypotheses. The assumed hydrogen source terms are shown on the figures 1 and 2. The air ingress into the vacuum vessel occurs at the same time as the hydrogen release. Assuming sonic flow conditions at the break (160 mm diameter hole), the air mass flow rate is 4.686 kg/s at 25°C. The scenario has been computed using the CAST3M-ITER code in order to assess the hydrogen distribution and combustion.

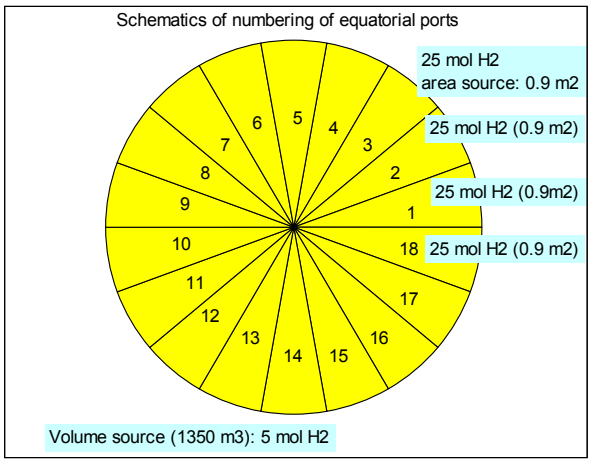

Figure 1 : H_2 from ITER equatorial ports

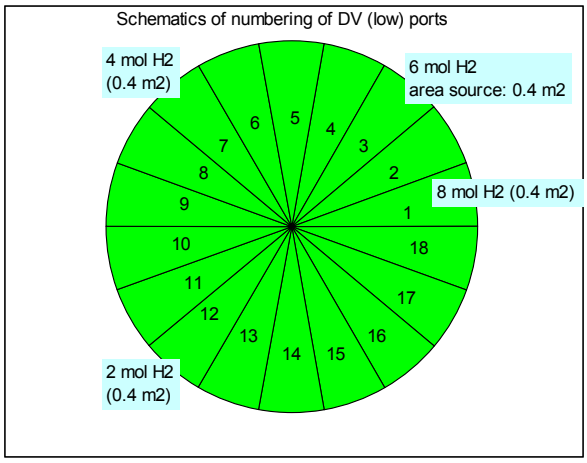

Figure 2 : H_2 from ITER lower ports

Hydrogen distribution: the figure 3 shows the zones where the concentration of hydrogen is greater than 4% (lower flammability limit of a hydrogen/air mixture) at the beginning of the transient. The hydrogen tends to concentrate at the top parts of the vacuum vessel (VV). In the ports through which it flows before reaching the VV, stratification is observed. The figure 4 shows the time evolution of the hydrogen cloud inside 4 %, 8 %, 10 % and 12 % isosurfaces.

Thanks to the quite fast dilution, the hydrogen concentration is lower than the flammability limit after 90 s.

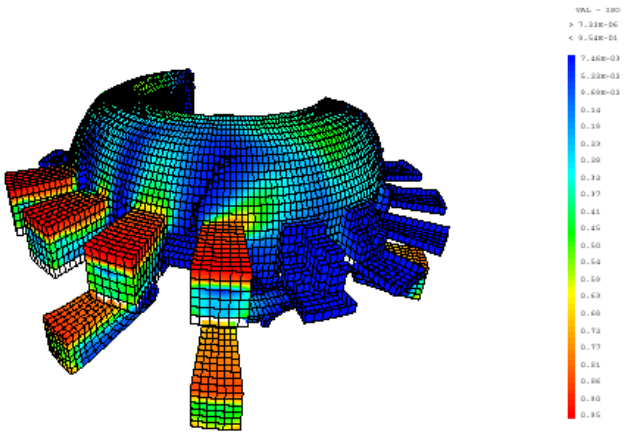

Figure 3 : H_2 molar fraction situation greater than 4 %vol at 10 s

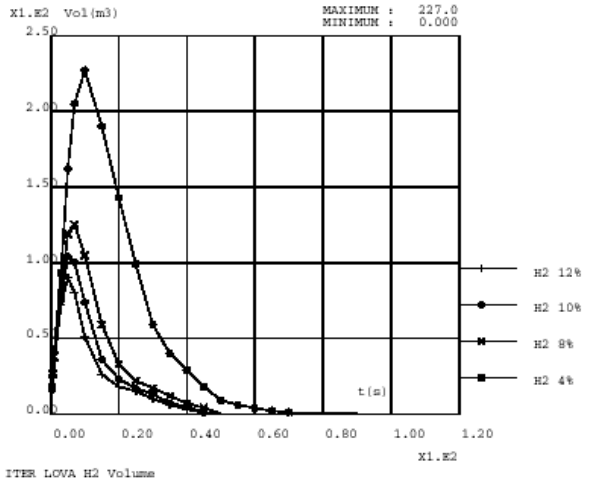

Figure 4 : H_2 cloud volume evolution with time

Hydrogen combustion: the combustion is calculated taking into account the results of the distribution calculations. Due to the low pressure in the VV, no flame propagates using the Arrhenius law. Thus, the CREBCOM model [1] is used. A conservative approach consists of assuming that all the hydrogen is burnt using this model. An envelope value of the impulse is obtained: 0.6 Pa.s. The figure 5 shows the time evolution of the highest pressure within the VV and the ports. One pressure peak reaches 3 bar.

CONCLUSIONS

The hydrogen risk in ITER during a LOVA situation is analysed. Due to a fast dilution the risk can exist only during a short time. Very conservative hypotheses, imposing the propagation of the flame despite the low pressure, lead to the occurrence of a pressure peak of 3 bar. Further R&D work on combustion at low pressure will allow to consider more realistic hypotheses in the next future.

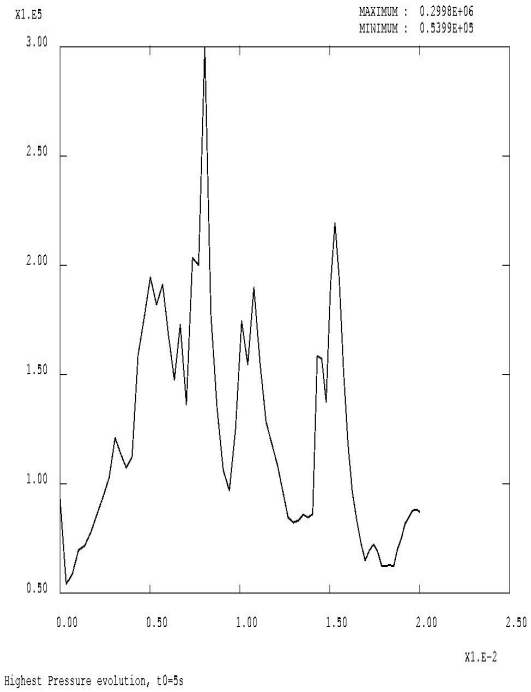

Figure 5 : Highest pressure evolution with time

REFERENCES

[1] Efimenko, Dorofev, CREBCOM code system for description of gaseous combustion, technical report Moscow, Russian Research Center Kurchatov Institute, 1998.

REPORTS AND PUBLICATIONS

F. Dabbene, ITER accident analysis: loss of vacuum through one VV/cryostat penetration line, CEA report SFME/LTMF/RT/03-037/A.

TASK LEADER

Pierre SARDAIN

DEN/DER/SESI/LESA
CEA-Cadarache
F-13108 Saint Paul Lez Durance Cedex

Tél. : 33 4 42 25 37 59
Fax : 33 4 42 25 36 35

E-mail : pierre.sardain@cea.fr

TW1-TSS-SEA5
TW3-TSS-SEA5.5-D03

Task Title: VALIDATION OF CODES AND MODELS - EVITA PAX ITR 2 Third set of calculation on the EVITA facility (cryogenic complementary tests)

INTRODUCTION

In the frame of the validation and verification of the codes used for ITER safety demonstration, a benchmark is under progress between the different parties of the project.

The aim of this benchmark is to compare experimental tests achieved on the EVITA facility and calculations performed by different pressurisation codes (CONSEN, PAX ITR, MELCOR, MAGS).

The results given by PAX ITR 2 (thermal-hydraulics computer code for spot calculations) for this set of post calculations are presented below. These studies have been conducted under ISO 9001 Quality Assurance procedures.

2003 ACTIVITIES

The objectives of the EVITA facility are:

- to investigate the pressurisation rate and heat transfer characteristics of water injection into the vacuum vessel of ITER when a cryostat event occurs (cf. GSSR, Vol. VII),
- to study the effects of this injection on the cryopump of the vacuum vessel,
- to participate in the codes validation and qualification, which is necessary in the frame of the ITER safety studies.

EVITA FACILITY MAIN FEATURES (cf. [2])

The experimental device is made of two main vessels:

- the pressuriser, which provides either steam or liquid water ($7.5 \leq P \leq 40$ bars, $T = 165°C$),
- the vacuum vessel.

The vacuum vessel structures are electrically heated in order to control the external temperature of the walls. A deflector plate is added to prevent a direct jet impingement on the cryogenic plate. This deflector plate is also heated.

The cryogenic plate is placed inside the test chamber (vacuum vessel). It is a copper plate 20 mm thick, with ∅ 6 mm holes fed with nitrogen.

The present set of calculations performed with PAX ITR code concerns steam or liquid water injections in presence of a cryogenic plate (Cf. following table 1).

Table 1 : Initial tests conditions

"Cryogenic condensation"				
Test n°	Wall temperature (°C)	Steam flow rate (g/s) at: 7.5 bar, 165°C	Water flow rate (g/s) at: 9 bar, 165°C	Water flow rate (g/s) at: 40 bar, 165°C
5.1	25°C	0.7	-	-
5.2	25°C	-	-	2.35
5.3	165°C	0.7	-	-
5.4	165°C	-	-	2.35
5.5	165°C	2.6	-	-

MODELLING OF THE EVITA EXPERIMENT

The EVITA facility modelling consists of a volume characterized by its height and structures. The injected flow rate and energy are imposed. The cryogenic plate (cf. figure 1) is modelled by a structure made of two layers (copper and ice). On the external side, the heat exchange coefficient with the nitrogen (-196°C) is imposed in the data set. On the internal side, the heat exchange depends on the ice thickness. The coefficient is calculated through a correlation. For condensation, this heat transfer coefficient (hint) is calculated through a Nusselt correlation (liquid film on a cold surface):

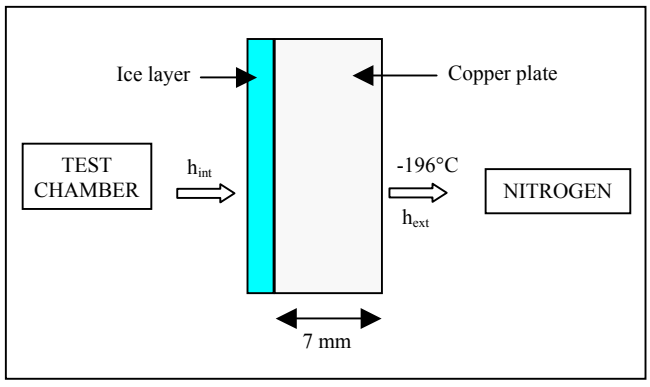

Figure 1 : Cryogenic plate modelling

PRELIMINARY WORK ON PAX ITR 2 COMPUTER CODE

In 2003, some improvements were made on the PAX ITR 2 computer code (cf. [4]). The most important work was carried out on the cryogenic structure.

To model a cryogenic plate, a specific development was performed to evaluate the kinetics of the pressurisation and the ice growth in the EVITA experiment. As the first results obtained were not completely satisfying (cf. [1]), it was decided to improve the programming the cryogenic structure, especially the convergence criterion.

RESULTS OF THE PAX ITR 2 CALCULATIONS

The aim of the calculation is to obtain a realistic pressurisation rate and ice growth. Post-tests results (pressurisation of the vessel and ice layer) have shown that steam injections (tests 5.1, 5.3, 5.5) can be well represented thanks to a corrective coefficient defined as an efficiency of the cryogenic plate. This efficiency factor takes into account different parameters like a geometrical factor and variations of ice properties (acting directly on the heat exchange coefficient). It limits the energy that could be removed by the plate as the present form of the Nusselt correlation over-estimates the energy absorbed by the cryogenic plate.

Concerning the liquid injection tests (tests 5.2 and 5.4), the calculations performed have emphasized the necessity to improve the flashing phenomenon modelling (to obtain a bigger amount of steam available for condensation on the cryogenic plate) and the structures heaters modelling (to have a constant wall temperature). This supposes that the average power of heaters is known.

Like in the previous campaign, some non-equilibrium phenomena have been noticed and cannot be represented by PAX ITR (cf. test 5.1).

CONCLUSIONS

Finally, EVITA PAX ITR 2 calculations are globally satisfying. Some identified improvements could be done for the next campaign to obtain a better modelling of EVITA transients.

Test 5.1 results are partly presented in the following table 2 and further results are reported in [3].

Table 2 : Test 5.1 - Comparison of parameters resulting from the ice growth

	Ice final thickness	Ice final mass	Liquid mass at the end of injection	Mean power removed by Nitrogen
Experiment	1.9 mm	173 g	105 g	945 W
Calculation	1.96 mm	179 g	143 g	1.09 kW

REFERENCES

[1] EVITA PAX ITR 2 – Second set of calculation on the EVITA facility (cryogenic condensation tests and cryogenic pressurisation tests)
TA-284722 Ind.A

[2] EVITA: Experimental results of EVITA cryogenic complementary tests
DER/STR/LCET 03/021

REPORTS AND PUBLICATIONS

[3] EVITA PAX ITR 2 – Third set of calculation on the EVITA facility (cryogenic complementary tests)
TA-341262 Ind.A

[4] PAX ITR 2 evolutions in 2003
TA-341264 Ind.A

TASK LEADER

Louis-Bertrand MARIE
in collaboration with CEA-Cadarache DEN/DER/SERI

TECHNICATOME
EP/DM/THN
Boîte Postale 34000
F-13100 AIX EN PROVENCE

Tél. : 33 4 42 60 28 43
Fax : 33 4 42 60 25 11

E-mail : louis-bertrand.marie@technicatome.com

TW1-TSW-002

Task Title: WASTE AND DECOMMISSIONING STRATEGY

INTRODUCTION

In the framework of waste management strategy, it has been demonstrated that one way to reduce the high level waste is detritiation. The knowledge of mechanisms involving in tritium trapping and desorption will allow to choose the most appropriate procedure. The working program deals with the management of tritiated steels and the way to reduce tritium transfer. This work is divided into 4 tasks:

- Task 1: Lowering of desorption kinetics of the residual tritium.
- Task 2: Lowering of the residual tritium concentration.
- Task 3: Validation of tritium loading technique in solid phase.
- Task 4: Role of microstructure on the tritium desorption.

This action is planned to finish in 2004. In 2003, only the task 1, 3 and 4 have been undertaken.

The tasks 1 and 3 use ingots from CEA Valduc. These ingots are obtained by melting under vacuum of waste composed with tritiated austenitic stainless steels.

2003 ACTIVITIES

The goal of the first task is to develop thermal treatment in solid phase to:

- Lower the residual tritium concentration (by desorption reheating).
- Reduce the diffusivity of residual tritium (by changing the microstructure).
- Reduce the kinetic of residual tritium desorption (by forming of barrier films).

Several conditions of thermal treatment (heating temperature, heating time, atmosphere) and surface state have been tested. For each conditions the surface activity, the residual tritium desorption of residual tritium at ambient temperature and the residual tritium concentration in steel have been evaluated. The procedure used to measure the activity surface, the desorption flux and the desorbed tritium quantity are the following:

- Immersion of steel samples during 30, 60 and 1000 minutes and liquid activity determination by scintillation by sampling at different time.
- For each steel sample, the analysis are done before and after reheating and after removal of oxidation layer.

The main results are given by the figure 1.

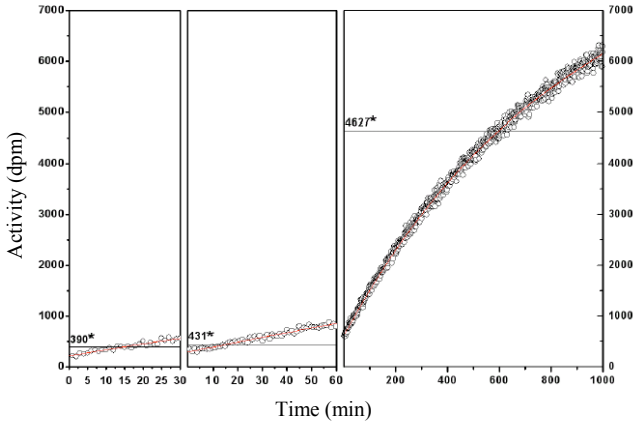

Figure 1 : Example of desorption curves during a sequence of 3 successive measures (30, 60 and 1000 minutes)

For the thermal desorption, the samples are reheated in silica sealed fial under primary vacuum at a temperature between 100 and 600°C during 20 h. In some case the comparison with a reheating at 300°C during 100 h has been done.

The residual tritium has been measured before or after reheating (and burnishing) after complete dissolution with aqua regalis.

The results are given by the figures 2 and 3.

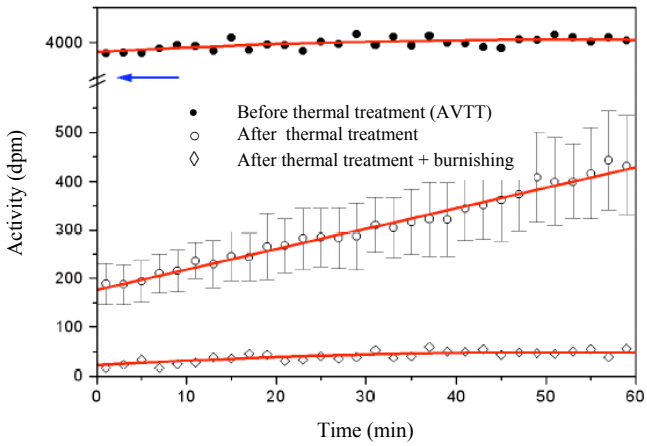

Figure 2 : Profiles of desorption plotted during 60 min on one sample : before reheating, after reheating (oxidized surface) and after reheating and burnishing of the surface

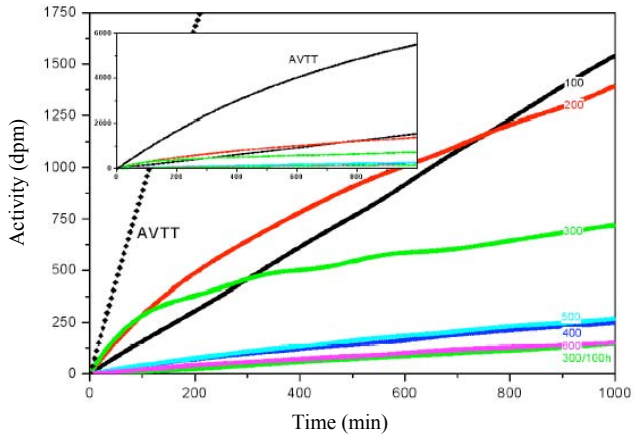

Figure 3 : Evolution of desorption profiles at different reheating temperatures (burnished surface after reheating)

The figure 2 shows that after reheating, the surface activity of the oxidized sample is very high and the desorption low. After burnishing, the activity and the desorption are low.

The figure 3 shows that a reheating of 20 hours at 100°C is sufficient to highly reduce the tritium desorption at ambient temperature.

For reheating temperature below 600°C, the surface activity is upper by 1 or 2 orders of magnitude compared to the non reheated samples. It demonstrates the presence of oxidation layer with a high tritium content. Some experiments have shown that this tritium is weakly linked and can easily transfer to a liquid phase.

Moreover, after 20 hours of reheating (300°C –400°C) the surface activity is highly reduced (80 %).

Considering the desorbed tritium, a reducing factor of 25 (compared with no reheating) can be reached with a reheating at a temperature upper than 300°C.

The kinetic of desorption is reduced by a factor 40 to 50 with a reheating at the temperature of 400°C and a duration of 20 hours.

The second part of this study was focused on the determination of oxide layer effect on the tritium desorption kinetic. To emphasize the oxide layer formation, the reheating has been done under wet air. The table 1 presents the apparent diffusion coefficient at 20°C.

Table 1 : Apparent coefficient diffusion at 20°C determined from desorption at 20°C during 1000 min

Material	Apparent diffusion coefficient at 20°C ($cm^2.s^{-1}$)
Non reheated sample	$4.1.10^{-12*}$
400°C, 15 min	$2.2.10^{-14}$
Reheated + burnished	$1.7.10^{-12}$
Literature reference [2]	$1.5.10^{-12}$

The task 3 has started : a loading technique is under evaluation. This technique is based on the electrolysis at 150°C of a molten salt ($NaHSO_4$, HTO (53.5 %), $KHSO_4$ (46.5 %)).

The task 4 will allow to study the effect of the microstructure. The characterisation of the reference material has been performed. The first experiments, such as influence of grain size reduction, on tritiated materials are under progress.

CONCLUSIONS

This work has demonstrated the influence of oxide layer in term of tritium desorption. Repetitive heating treatments can highly reduce the desorption kinetic. The tempearture to reach and the duration of the treatment are rather low and allow to envisage such processing for a waste treatment.

The continuation of this work will consist in lowering the residual tritium concentration. Before that, a method for tritium loading has to be validated.

The understanding of the microstructure role on the tritium desorption will allow to propose an adapted solution to the management of tritiated waste either by facilitating the desorption by a heating treatment or by fixing the tritium inside the bulk.

REPORTS AND PUBLICATIONS

[1] A. LOSSOUED, A-M. BRASS, J. CHENE - Interim report on task TW1-TSW-002, Décember 2003.

[2] P. TISON, Influence de l'hydrogène sur le comportement des métaux, rapport CEA R-5240, 1984.

TASK LEADER

Olivier GASTALDI

DEN/DTN/STPA/LPC
CEA-Cadarache
F-13108 Saint Paul Lez Durance Cedex

Tél. : 33 4 42 25 37 87
Fax : 33 4 42 25 72 87

E-mail : olivier.gastaldi@cea.fr

TW3-TSS-SEA5.3

Task Title: ICE FORMATION ON CRYOGENIC SURFACES

INTRODUCTION

The computer codes which are used for the analysis of the accidental sequences in ITER should have good quality assurance level. The experimental program EVITA allows to simulate the physical phenomena occurring during a steam or water ingress in the cryostat and in the vaccum vessel in presence or not of non condensable gas, which is one of the identified accidental sequence in the ITER safety report.

The main experimental results are the pressure evolution in the vacuum vessel, the different heat exchanges and the ice formation on the cryogenic surface.

2003 ACTIVITIES

The EVITA experiment (figure 1) mainly consists in a vacuum vessel in which pressurized water or steam can be injected. The inner walls of the vessel can be heated to a given temperature. A cryogenic plate connected to a liquid nitrogen loop (77 K) is located inside the vacuum vessel.

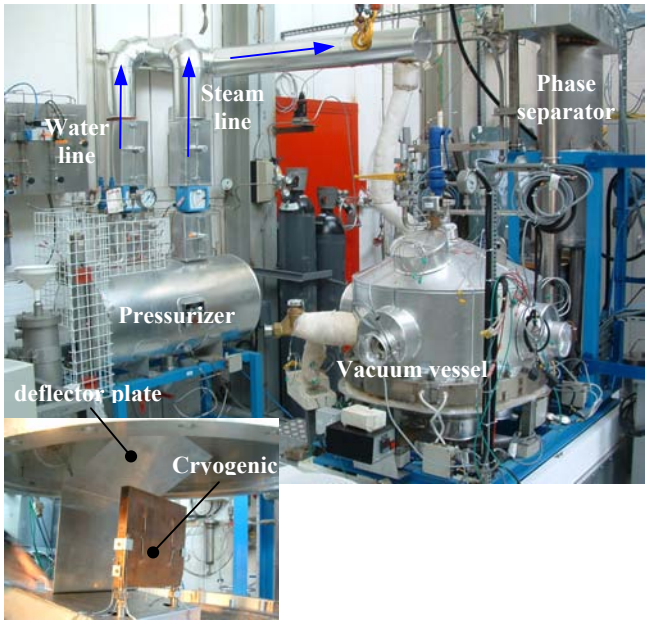

Figure 1 : View of the EVITA facility

ANALYSIS OF CRYOGENIC TESTS

The analysis of the cryogenic tests performed during year 2002 [1] had allowed to understand phenomena occurring in the vacuum vessel.

Therefore some modifications of the facility have been decided to improve the ice formation on the cryogenic plate:

- a deflector plate has been put in place (figure 1) to avoid the direct impact of the steam/water jet on the cryogenic plate in the vessel,
- the steam and water flow rate have been reduce by 2/3,
- there was no more fluxmeter on the cryogenic plate,
- the coriolis flowmeter was removed.

Five complementary cryogenic tests have been decided in the frame of a benchmark with the EFDA participants and been performed during the first part of the year.

An ice layer was formed on the cryogenic surface during each test (figure 2). A method to evaluate the amount of ice was set up.

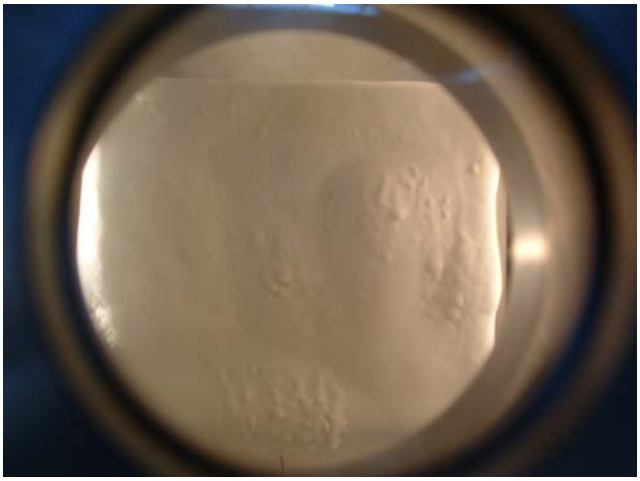

Figure 2 : View of the cryogenic plate with the ice layer formed on it

The vacuum vessel pressure evolution during these tests with ice formation was characterized (figure 3).

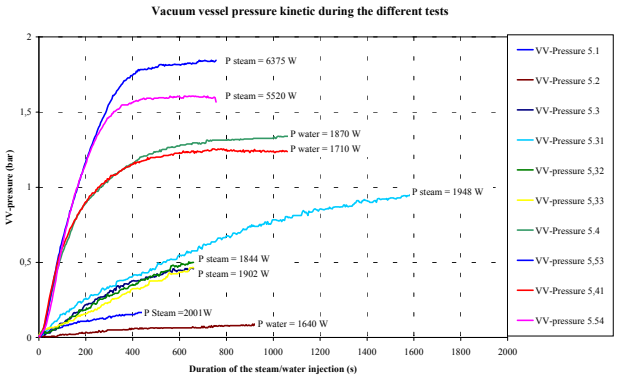

Figure 3 : Pressure evolution in the vacuum vessel

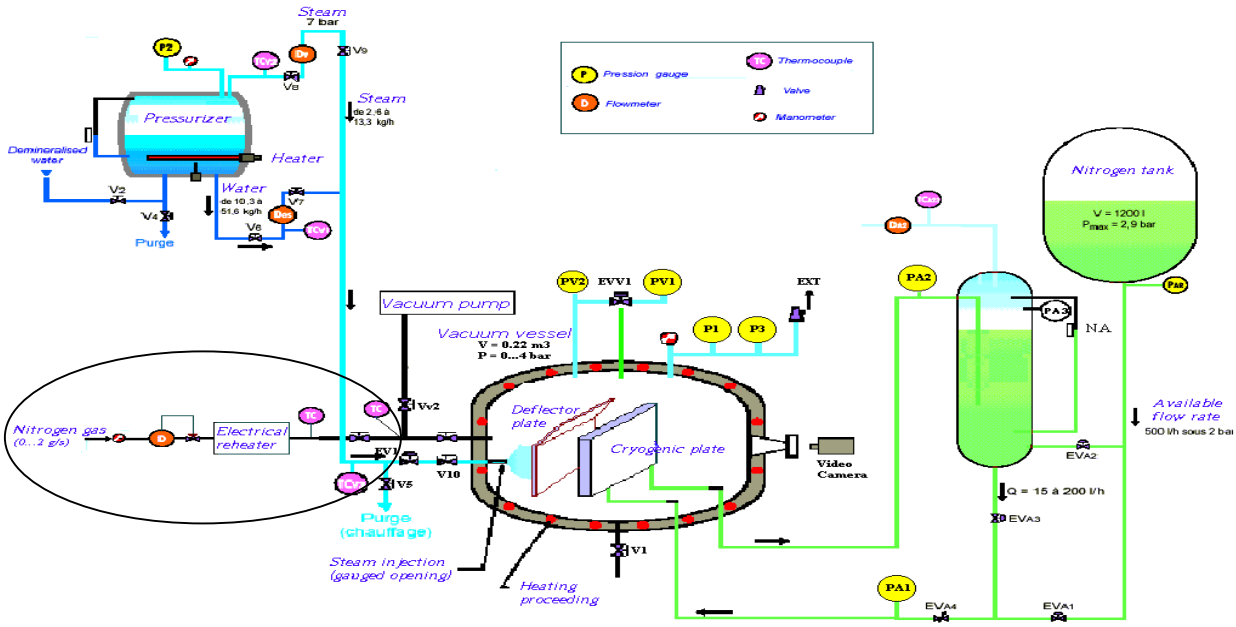

Figure 4 : Flow diagram of the EVITA facility with the new nitrogen gas injection

MODIFICATIONS OF THE EXPERIMENT

During the second part of the year the EVITA facility was modified to prepare the next test campaign concerning the study of the simultaneous incondensable gas and water/steam ingress in the vacuum vessel (figure 4).

The injection of nitrogen gas has been set up on the EVITA facility. To obtain nitrogen gas at a temperature of 165°C with a 2 g/s flow rate, a re-heater has been implemented in the injection line.

The different experiments performed on the EVITA facility have shown that the re-heater was able to heat nitrogen gas at 165°C with a flowrate range from 0.2 to 2 g/s. The gas flowrate is controlled by a mass flowmeter with its associated electrical regulated valve. Measurement of the gas flowrate is available on the monitoring data system.

Several tests of simultaneous steam and gas injections have been realized in the vacuum vessel. We have not notice any problem during these tests.

The feasibility of the experimental program with non condensable gas in the expected range is demonstrated.

CONCLUSIONS

The analysis of the tests performed in 2002 has given important informations (pressure evolution, ice layer formation) on the different phenomena occurring in the vacuum vessel during water or steam ingress.

The complementary tests, performed during the first part of the year, after this analysis have confirmed this analysis. During these tests an ice layer was formed (from 170 g to 470 g) on the cryogenic plate.

The second part of the year was devoted to set up the incondensable gas injection on the EVITA facility. Thus, several tests have been realized to demonstrate the feasibility of the experimental program.

REPORTS AND PUBLICATIONS

[1] L. Ayrault, J. Hiltzer, “Analysis of the results of the first EVITA tests with the cryogenic plate”, CEA report DER/STR/LCET 03/005.

[2] L. Ayrault, F.Garnero, “Study of non condensable gas injection experiments in the EVITA facility”, CEA report DER/STR/LCET 03/006.

[3] L. Ayrault, F.Challet, “EVITA : Experimental results of EVITA cryogenic complementary tests”, CEA report DER/STR/LCET 03/021.

[4] L. Ayrault, “Preparation of the cryogenic tests with steam in presence of non condensable gas”, CEA report DER/STR/LCET 03/035.

TASK LEADER

Laurent AYRAULT

DEN/DTN/STPA/LTCG
CEA-Cadarache
F-13108 Saint Paul Lez Durance Cedex

Tél. : 33 4 42 25 44 72
Fax : 33 4 42 25 66 38

E-mail : laurent.ayrault@cea.fr

JW3-FT-3.14

Task Title: LASER TRITIUM DECONTAMINATION

INTRODUCTION

The retention and the excessive content of hydrogen isotopes in plasma-facing components present a severe problem for a proper design of a future thermo-fusion reactor as these factors may affect dramatically the reactor operating regimes. Thus, the dehydrogenization of installation components is regarded as one of the crucial problems in a future thermo-fusion reactor design and construction. For ITER vacuum chamber, the maximum acceptable tritium inventory is estimated as about 300 g. The JET experimental results extrapolation on ITER installation demonstrated that this maximum tritium value is reached with less than 100 shots [1].

Among many various methods that were suggested for plasma-facing components detritation, one should mention the use of lasers that may provide the concentration of a high energy flow on the contaminated surface of the installation [2, 3]. A fast heating of an exposed surface by the laser beam allows to obtain the temperature higher than 1000 K on a thin (1 – 100 μm) near-surface layer, thus, resulting in detritation either by hydrogen desorption from the surface or by ablation of this near-surface layer.

The visible and near-IR Nd-YAG lasers with 100 ÷ 500 W average power that can be transmitted by optical fibers may provide a completely automatic unattended system for surface cleaning in a vacuum chamber of a reactor. This report presents the experimental results on graphite detritation by laser heating and ablation obtained with the experimental installations developed in DPC/SCP (CEA Saclay) for studies on graphite tritium decontamination with repetition rate nanosecond Nd-YAG lasers.

2003 ACTIVITIES

LASER ABLATION

The laser ablation measurements were performed on both the plasma-facing surface (TORE SUPRA and TEXTOR samples) with a co-deposited layer and on the opposite tile side that was not suffering the plasma effect (pure graphite).

A low repetition rate laser ablation of a polished pure graphite surface with a homogenized laser beam (Quantel, 4-10 ns pulse duration, 532 nm) was under study. A typical crater form obtained with the homogenized beam is presented on figure 1.

The crater depth was determined to be a linear function of the number of applied laser shots (figure 2).

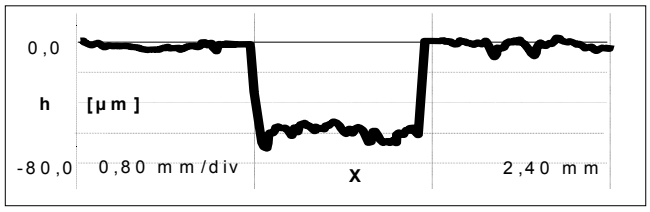

Figure 1 : Typical crater form obtained with a homogenized laser beam

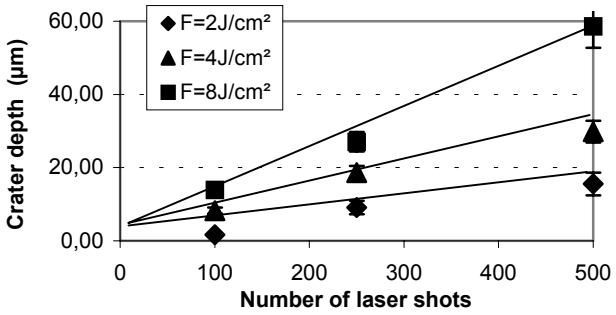

Figure 2 : Pure graphite crater depth as a function of laser shots for three different laser fluencies

It was found valid for different laser fluencies (2, 4, and 8 J/cm^2) and for the crater depth up to 60 μm.

The crater depth (figure 3) was also found to be of a linear dependence from the laser fluency up to 5 J/cm^2.

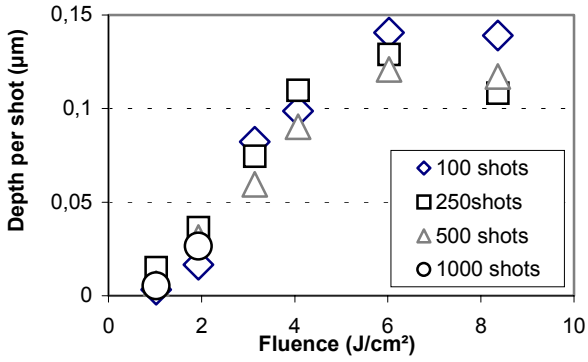

Figure 3 : Pure graphite crater depth (normalized to one laser shot) as a function of laser fluency for a different number of laser shots applied for the crater formation

The ablation of TEXTOR graphite with a thick co-deposited layer was studied with low- and high-repetition rate lasers (figure 4).

The co-deposited layer ablation efficiency (0.2 μm/J cm^{-2}) was determined to be approximately ten times higher than that of graphite (0.025 μm/J cm^{-2}).

Given the obtained co-deposited layer ablation efficiency (η = 0.2 μm/J cm^{-2}), we can estimate the performances of laser surface cleaning:

S (m^2/hour) ≅ **0.36** η (μm/Jcm^{-2}) **P** (W) / **h** (μm)

where: P(W) - a mean laser power, and h(μm) – a co-deposited layer depth. Thus, with a laser of 500 W mean power, approximately 0.9 m^2 of co-deposited layer of 40 μm thickness could be ablated within an hour.

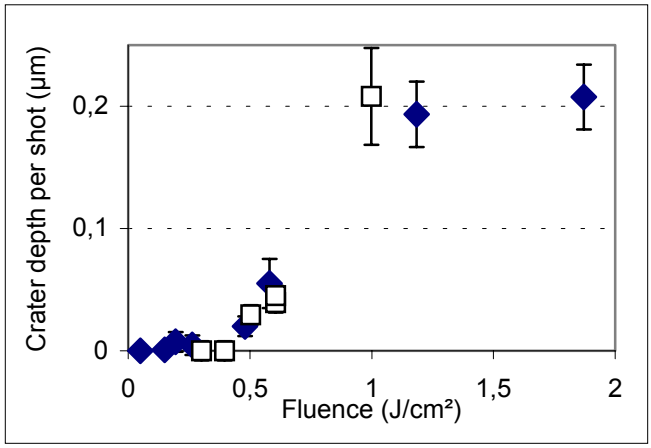

Figure 4 : Crater depth versus laser fluency obtained in air (1 atm) with a thick co-deposited layer from TEXTOR. (□) – low repetition laser (4-10 ns pulse duration, 532 nm, homogenized beam, 20 Hz repetition rate; (◆) - high repetition rate Nd-YAG laser (100 ns pulse duration, 532 nm, homogenized beam, 10 kHz repetition rate)

LASER ABLATION THRESHOLDS FOR GRAPHITE AND FOR CO-DEPOSITED LAYER

Laser ablation threshold fluency F_{th} (J·cm^{-2}) was found to distinguish two different regimes of a pulsed laser beam interaction with a solid. For the laser fluencies $F < F_{th}$, the laser beam was observed only to heat the near-surface layer without any visible damages or effects on the surface. The surface temperature was lower than the solid melting or sublimation temperature.

Thus, with the laser fluency $F < F_{th}$, we can avoid the graphite surface destruction during its detritation. With a high laser fluency ($F > F_{th}$), the laser beam was observed to ablate the surface with the rate being determined by laser fluency, surface matter properties, and environmental conditions. Thus, the experimental determination of the laser threshold fluencies for graphite samples with a co-deposited layer is regarded essential to distinguish the laser ablation and heating regimes and, hence, to control laser detritation.

The experimentally obtained crater depths versus laser fluencies (figure 3 and figure 4) allowed to obtain the ablation thresholds for graphite and for a co-deposited layer. The pure graphite laser ablation threshold was determined to be 1 J/cm^2 , while for a TEXTOR co-deposited layer it was found to be lower : F_{th} = (0.4 ± 0.1) J/cm^2.

DETRITATION BY PULSED LASER HEATING

Laser ablation thresholds for a co-deposited layer and for pure graphite surfaces were obtained experimentally and applied in laser heating detritation experiments with TORE SUPRA samples with a co-deposited layer. Laser fluencies were adjusted to be lower than the laser ablation threshold (0.4 Jcm^{-2}) obtained for co-deposited TEXTOR samples. The Glow Discharge Optical Spectroscopy method (GD-OS method) was applied for in-depth analysis of graphite samples. Figure 5 (a)-(c) presents the results obtained.

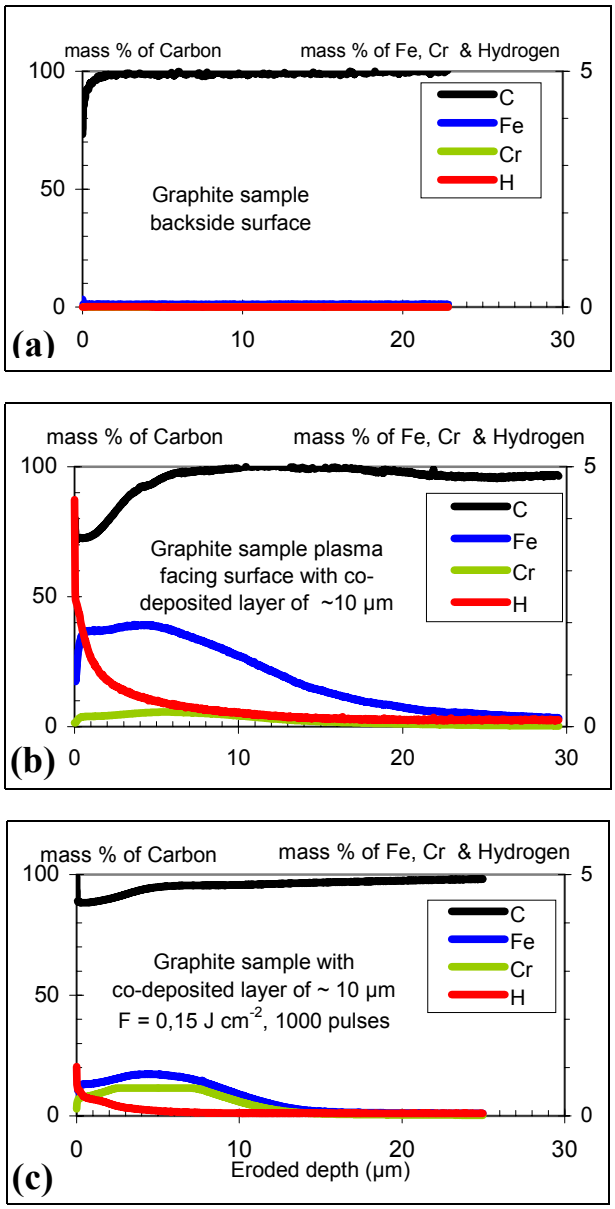

Figure 5 : TORE SUPRA co-deposited layer in-depth analysis by GD-OS method

The GD-OS method was applied to analyze three zones of a graphite sample: the backside graphite surface without a co-deposited layer - figure 5 (a); the graphite surface with a co-deposited layer without laser treatment - figure 5 (b); the graphite surface with a co-deposited layer with application of the laser beam with the fluency lower than the ablation threshold fluency for a co-deposited layer - figure 5 (c).

The GD-OS measurements gave the following qualitative co-deposited layer analysis. The graphite backside surface was found free from impurities (figure 5 (a)). In a co-deposited layer, the impurity concentration was determined to decrease with the increase of the intensity of the surface treatment by a laser beam.

Thus, hydrogen isotopes (H+D) concentration by in-depth measurements of the GD-OS method demonstrated a significant decrease in hydrogen spectral line intensity for the co-deposited layer zones exposed to laser heating. Given these preliminary results, the conclusion can be made that a co-deposited layer heating by nanosecond laser pulses can be applied for graphite surface detritation.

CONCLUSIONS

Low and high repetition rate laser benches with a sufficiently complete control and measurement equipment were developed and applied for graphite heating and ablation studies. The ablation thresholds for graphite ($\cong 1$ J cm^{-2}) and for co-deposited layer ($\cong 0.4$ J cm^{-2}) surfaces were determined experimentally. In our studies on laser ablation of graphite samples from TORE SUPRA (CEA Cadarache) and TEXTOR, different ablation efficiencies - (0.025 µm/J cm^{-2}) for graphite and (0.2 µm/J cm^{-2}) for a co-deposited layer were obtained.

The obtained ablation efficiency was estimated to allow a 40 µm thick co-deposited layer ablation with the rate of $\cong 1$ m^2 per hour with 500 W laser power. Different ablation thresholds and laser ablation efficiencies for graphite and a co-deposited layer could be applied to ensure self-control of laser surface cleaning. Thus, for a co-deposited layer removal with the laser fluency of F $\cong$ 1 J cm^{-2} (graphite surface ablation threshold), the minimum laser effect on the graphite surface could be ensured.

The feasibility tests carried out with GD-OS diagnostics demonstrated that heating by nanosecond laser was sufficiently efficient to perform detritation of thin co-deposited layers. The LA-OES method can be applied in real-time control of the co-deposited layer removal by laser ablation. It can also be used as in-vessel diagnostics to localize and to characterize co-deposition removal.Additional experimental study on laser heating and ablation with different types of co-deposited layers in controllable environmental conditions (gas composition, pressure) should be undertaken to provide supplementary data on detritation by laser heating and ablation. The theoretical model should be developed to compare the experimental results on the laser surface heating and ablation with the simulation data. These investigations seem to be essential to obtain both the optimal interaction regime and to improve the laser detritation method performances.

REFERENCES

[1] R. A. Causey, J. Nucl. Mater. 300 (2002) 91-117.

[2] M. Friedrich, W. Pilz, G. Sun, R. Behrisch, C. Garcia-Rosales, N. Bekris, R.-D Penzhon, Nucl. Instrum. Methods B, B161 – 163 (2000) 216-220.

[3] C.H.Skinner, H. Kugel, D. Mueller, B.L.Doyle, W.R. Wampler, "Tritium Removal by CO_2 laser heating", Proceedings of SOFE'97, CH 36131 Vol. 1 (1998) 321.

REPORTS AND PUBLICATIONS

Laser Decontamination Tritium Removal - F. Le Guern et al - Report CEA, DEN/DPC/SPA/LLA/NT/2003-0.

Graphite Detritation by Nanosecond Laser Pulses - A. Semerok, J.-M. Weulersse, F. Brygo, Ch. Lascoutouna, Ch. Hubert, F. Le Guern, M. Tabarant - Report CEA, DEN/DPC/SCP/LILM/NT2004.006, 2004, 35 pages.

TASK LEADERS

A. SEMEROK, JM. WEULERSSE, F. LE GUERN

DEN/DPC/SCP/LILM
CEA-Saclay
F-91191 Gif-sur-Yvette Cedex

Tél. : 33 1 69 08 65 57
Fax : 33 1 69 08 78 84

E-mail : asemerok@cea.fr

JW0-FT-2.5

Task Title: DEDICATED PROCEDURES FOR DETRITIATION OF STEEL AND GRAPHITE

INTRODUCTION

Studies have been performed to determine different processes that could be used for tritium removal. The aim of this paper was, to study, at laboratory scale, different procedures which may be used for carbon materials and stainless steels detritiation.

Thermal detritiation kinetics till 1300 K has been studied under various atmospheres; full chemical dissolution of samples has also been performed both for graphite and steel, this to perfectly know the tritium content in such matrices. Finally a study of tritium content in steel layers has also been made, to learn about the tritium behaviour. All results are given, allowing the possibility to take a decision either for detritiation procedure or storage conditions. Future studies will be performed at higher temperatures (till melting in the case of steel) with an inductive furnace, however these studies are not included in this task.

2003 ACTIVITIES

After a bibliography study, it has been noticed that steel detritiation occurs from 573 K and above . Tritium diffusion is negligible when tritium is combined as HTO which is generated under air atmosphere at such a high temperature.

LPC laboratory has developed comprehensive procedures to extract tritium from steel; this has been performed by thermal outgassing under air atmosphere. To check the good detritiation level for analytical purposes, another procedure is currently under application : a full dissolution of steel sample with hydrochloric acid solution.

To perform this work, steel samples were originated from a French fast breeder reactor plant to be decommissioned.

TECHNICAL RESULTS

Analyses were performed on rather small quantities of steel, knowing that the radio-chemistry laboratory is presently limited in terms of radioactivity levels and safety regulation.

Weighed sample (about 700 g) was dropped in an hastelloy container which may be heated till 1323 K.

Detritiation of samples was performed in a furnace at 1273 K under controlled atmosphere.

Downstream the container a MARC 7000 ® system has been set to recover and convert tritium to tritiated water.

Detritiation was performed under two different atmospheres to check the behaviour of tritium species, and sampling was also performed at intermediate temperatures.

DISCUSSION

Some differences occur between air and hytec (5 % hydrogen in argon gas) atmospheres for total tritium extraction. With air the total tritium content is higher and HTO species is favoured; this is linked to a rapid chemical oxidation of tritium. With Hytec, a difference shows a lack of total tritium which may be related to a possible diffusion of tritium as HT in the metallic structure of Hastelloy, this is more important at temperature above 800 K ; a possible diffusion kinetics may occurs at high temperature.

Considering hytec atmosphere, a swamping effect may be observed which, by isotopic exchange with large amount of hydrogen, may favour tritium extraction.

Another observation may be underlined at 673 K, tritium species are HT (56 %) and HTO (44 %) ; one reason which may explain the presence of HTO is a possible presence of oxygen either in the microstructure of the bulk or at the surface as metal oxide (or both). This oxygen may react with tritium in situ and generate tritiated water. A very low oxygen concentration and the very low sensitivity of the radio-isotope measurement permits such a possible explanation.

A large amount of tritium is distributed within the first thin (less than 10 μm) layer; considering a thickness of 70 μm we may notice that it contains about 21 % of total tritium; this leads to a simple calculation: 21 % of tritium is present in 6.71 g of dissolved steel (i.e. 0.5 % of metal weight). Consequently this means that tritium concentration is depleted in bulk.

GRAPHITE

Concerning graphite, work has been performed on actual divertor sample from JET, JET samples have been tested and a methodology has been developed to fully oxidize graphite. This is a wet ashing procedure which enables the elimination of carbon as carbon dioxide species, tritium is also eliminated and distributed in different phases, depending upon the original form linked to graphite. This technique, different from dry ashing, allows the measurement of both chemical and radio-chemical impurities of graphite.

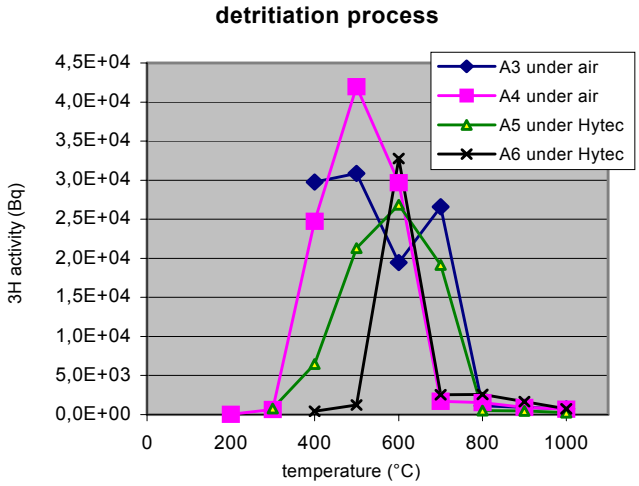

Four series of different graphite samples from first wall materials of JET facility were sent to develop different methods for tritium activity measurement; calculation of supposed activities has been performed by JET staff.

CHEMICAL PROCEDURE

A chemical destruction of graphite (called wet ashing), is performed with a cocktail of oxidising acids : fuming nitric acid and perchloric acid. The released gases are purged by air through a catalytic oxidation furnace and the produced water is collected in a cold trap containing some water in a bubbling device.

The acid phase is partially distilled to recover one part of tritium. Tritium species (HT and HTO form) are counted. This procedure allows the treatment of 20 g of graphite which can be fully oxidized using about 100 mL of acidic cocktail. The calculated tritium activity for the old TFTR graphite samples is about 30 Bq/g and the measured activity is around twice higher: 66 Bq/g

THERMAL PROCEDURE

The same method as steel detritiation is applied for the graphite JET samples from MKIIA divertor tile (10N8 after the DTE1 campaign). Detritiation was performed under two different atmospheres to study the behaviour of tritium species. To measure the detritiation kinetics, sampling was performed by step every 100°C. Under air, practically all the tritium is oxidized to HTO, and CFC samples are oxidized to CO_2. There is no residual graphite in the reactor after the first step up to 1273 K. The second step at 1323 K is used to insure the elimination of residual tritium in the reactor.

In order to measure tritium species, we need hytec gas (Argon + 5 % H_2). With hytec, it is assumed that an isotopic exchange is possible between H and ^3H ; after the first phase until 1273 K, the same quantity of CFC still remain. To detritiate CFC or graphite without any destruction (absence of oxygen), hytec detritiation process must be used.

COMPARISON BETWEEN CHEMICAL AND THERMAL METHODS OF TRITIUM ACTIVITY MEASUREMENT

To compare both methods, the 4D-CFC KC11 baked A2 sample (recent TFTR sample) was cut in two parts an analysed using chemical and thermal method. This sample size was small and study was performed with sub-samples of 10.3 mg for thermal measurement and 19.6 mg for chemical measurement. The obtained results are:

23 ± 3 kBq/g with thermal procedure
18 ± 3 kBq/g with chemical procedure

Taking into account the very small analysed quantity in both cases and assuming a fairly good homogeneity, the obtained results have to be considered as equivalent. To make a more reliable validation, bigger samples are necessary, however we may consider that both methods lead to similar results.

CONCLUSION

For steel detritiation, secondary wastes as gas or liquid will be produced. It is essential to reach a compromise between the initial tritium concentration in the waste, the final tritium concentration in the waste and the volume of secondary wastes produced. Concerning carbon dust and flakes, full combustion seems to be the best detritiation process. Even if large quantities of secondary wastes are produced, this process can be selected because concerned volumes are low. Heating processes at lower temperatures are also promising because they allow tritium removal from surface and bulk. Moreover their application could be easier and cheaper. Nevertheless, before or after all these treatments, it is possible to have recourse to radioactive decay. During this period of interim storage, the tritium out-gasing can be controlled using specific packages and/or an atmosphere detritiation system of the facility. The developed procedures show the possibility to measure tritium in graphite or CFC with thermal or chemical method. The comparison of both methods displays similar results and permits a full tritium recovery. Thermal process under Hytec allows graphite detritiation without any destruction. Optimal detritiation temperatures are between 573 K and 1073 K.

TASK LEADER

Christian POLETIKO

DEN/DTN/STPA/LPC
CEA-Cadarache
F-13108 Saint Paul Lez Durance Cedex

Tél. : 33 4 42 25 64 93
Fax : 33 4 42 25 72 87

E-mail : christian.poletiko@cea.fr

UNDERLYING TECHNOLOGY PROGRAMME

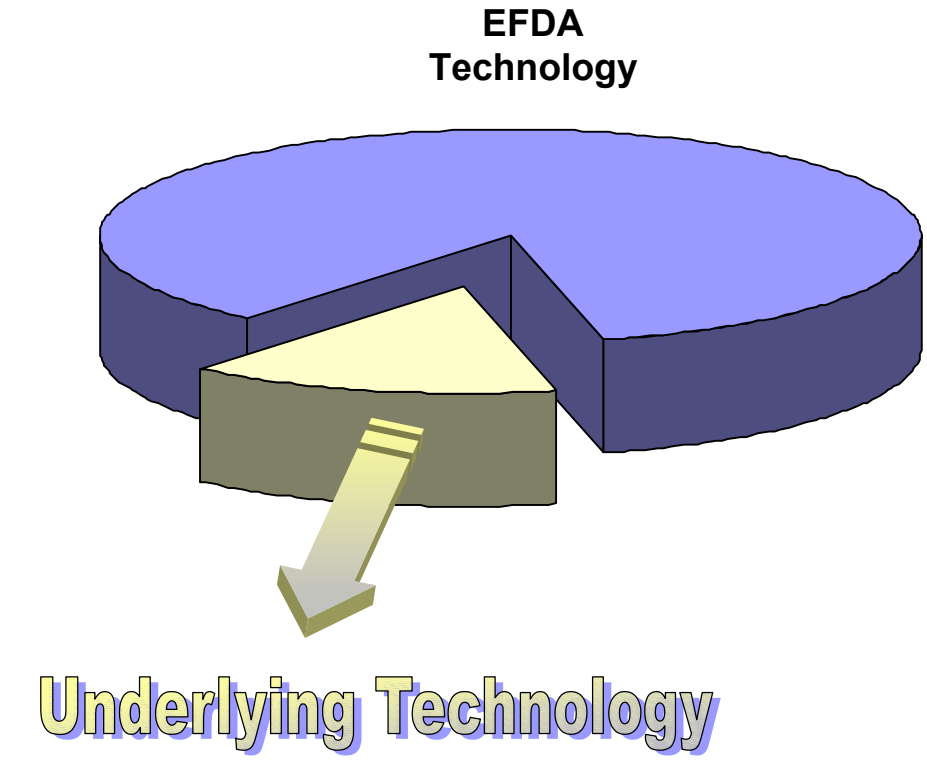

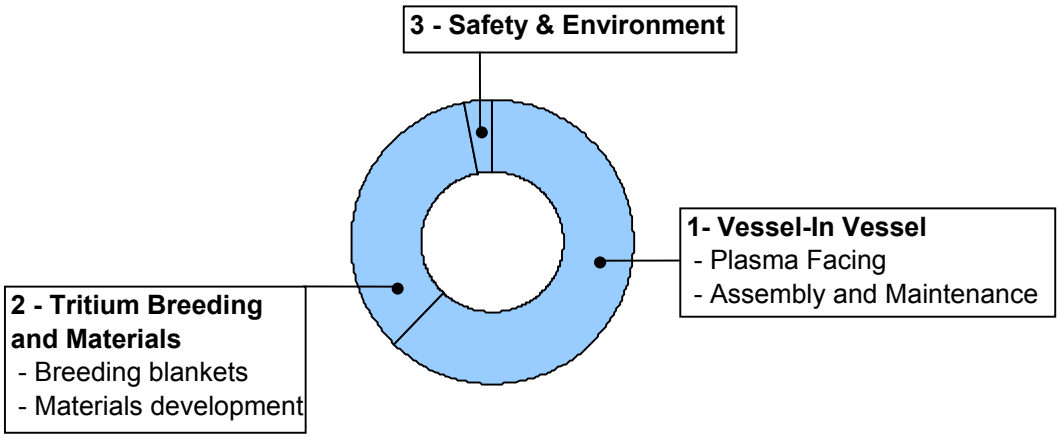

UT-S&E-LASER/DEC

Task Title: LASER DECONTAMINATION: TRITIUM REMOVAL

INTRODUCTION

The retention and the excessive content of hydrogen isotopes in plasma-facing components present a severe problem for a proper design of a future thermo-fusion reactor as these factors may affect dramatically the reactor operating regimes. The excessive tritium content on the reactor surfaces necessitates an extra radiation safety for the maintenance personnel. Thus, the dehydrogenization of installation components is regarded as one of the crucial problems in a future thermo-fusion reactor design and construction. Among various detritation methods that were suggested for plasma-facing components detritation, one should mention the use of lasers that may provide the concentration of a high energy flow on the contaminated surface of the installation.

A fast heating of an exposed surface by the laser beam allows to obtain the temperature higher than 1000K on a thin (1 – 100 μm) near-surface layer, thus, resulting in detritation either by hydrogen desorption from the surface or by ablation of this near-surface layer. The Nd-YAG lasers (cw or high repetition rate) with 100-500 W average power that can be transmitted by optical fibers may provide a completely automatic unattended system for surface detritation in a vacuum chamber of a reactor. The ablation with laser pulses of 10-100 nanoseconds duration can be applied for co-deposited layer destruction.

The aim of our studies was to discuss some theoretical models for graphite surface detritation by lasers. For detritation by IR and visible lasers with the pulse duration higher than some nanoseconds, the thermal mechanism is seen as the principal one. That is why the simulation of the surface heating by the focused laser radiation and some particular features and regimes of laser ablation where of our particular attention. Both the heating and the laser ablation of graphite are known to depend on its optical properties (absorption coefficient of the surface and its dependence from temperature) and thermo-physical properties (density, porosity, specific heat capacity, thermal conductivity). Some distinctive features of graphite surface detritation and the ways for laser detritation optimization are discussed in the conclusions.

2003 ACTIVITIES

SIMULATION OF SURFACE HEATING BY LASER

For a general case of a surface heating by a focused laser beam of a moderate intensity (a fundamental or a second harmonic of cw Nd-YAG lasers or pulsed repetition rate Nd-YAG lasers being focused into a spot of $2r_0 \sim 0.1$-1.0 mm diameter on the surface) with a pulse duration higher than 1 ns, the heat equation for the temperature T can be presented in the form [1]:

$$C(T)\frac{\partial T}{\partial t} = \mathrm{div}\left[K(T)\nabla T\right] + Q(t,r,z),$$

where $C(T)$ and $K(T)$ - specific heat and thermal conductivity of a solid. The laser heating-source term Q can be presented as: $Q(t,r,z)=I(t,r)A\alpha\exp(-\alpha z)$, where r and z - the cylindrical coordinates with the initial point on the surface of a solid and with the z-axis directed normally to the surface; $I(t, r)$ - the radial distribution of laser intensity (which is assumed to be distributed axially-symmetrically near the focus on the metal surface); A - the surface absorptance ($R = 1 - A$ is the surface reflectivity), and α - the laser absorption coefficient.

For the matters with a high absorption coefficient (graphite and metals, in particular), the laser energy penetration depth (the skin layer that is determined by $1/\alpha$) is usually much smaller than the laser spot radius (~ 1 mm, in our case) on the solid surface. It is also lower than the heat diffusion penetration depth $l_t = (D\times\tau)^{0.5}$ on the time scale of the laser pulse duration ($\tau \geq 10$ ns) with $D = K/\rho C$ - thermal diffusivity and ρ - solid matter density. With $\alpha r_0 >> 1$ and $\alpha l_t >> 1$, we deal with the surface heating of a solid (rather than its volume heating). In this case, the heat equation for the temperature T can be presented in the form, where the source term is omitted:

$$C(T)\frac{\partial T}{\partial t} = \mathrm{div}\left(K(T)\nabla T\right),$$

with the laser heating-source term being considered as a boundary condition:

$$-K(T)\left.\frac{\partial T(t,r,z)}{\partial z}\right|_{z=0} = AI(r,t),$$

For a quantitative estimation of the solid surface temperature, the numerical solution of the non-linear heat propagation equation with the temperature-dependent thermal parameters of a metal should be performed. Thus, it is necessary to know thermo-optical parameters of a solid (specific heat, thermal conductivity, surface reflectivity, laser absorption coefficient α) and its temperature dependences.

The analytical solution for the temperature of a solid may be obtained with the hypothesis that the thermo-optical solid parameters are independent from the temperature [1]. In this case, the temperature of the semi-infinite solid at the initial temperature $T=T_o$ heated by a constant heat flux $F(W/cm^2)$ at z=0 starting at t=0 is expressed as:

$$T(t,x) = T0 + \frac{2F}{K}\left\{\sqrt{\frac{Dt}{\pi}} \times \exp\left(-\frac{z}{4Dt}\right) - \frac{x}{2}\,\mathrm{erfc}\,\frac{z}{2\sqrt{Dt}}\right\}$$

Here, z - solid depth, K - thermal conductivity, D=K/ρC - thermal diffusivity, and 'erfc' - error function. From this equation, we can obtain the surface temperature $T(z=0)$ or the flux F necessary to raise the surface temperature by T degrees during time t:

$$T(t,z=0)=T0+\frac{2F}{K}\left\{\sqrt{\frac{Dt}{\pi}}\right\} \text{ or } F(Wcm{-}2)=(T-T0)K\sqrt{\frac{\pi}{4Dt}}$$

Both analytical and numerical heat propagation results were applied for the graphite heating by a cw-CO_2 laser beam [2]. The temperature relaxation time for a graphite layer of the depth "z" was found to be estimated by $\Delta t = C\rho z^2/2K$. For z = 100μm, ρ = 2.2 g/cm^3, C = 1.77 J/g K (at 400K), K = 0.082 W/cm K (at 400K), the temperature of 100 μm thick layer was observed to relax with the characteristic time of 5 ms. Preliminary numerical simulations of the solid surface heating by the laser beam were under study in DPC/SCP/LILM (CEA Saclay). On the first stage, a simple one-dimensional model was made to estimate the thermal behaviour of a matter during and after energy deposition, with thermal diffusivity and conductivity being taken into account. The simulation was based on a numerical solution of the simplified heat equation for a solid surface of infinite thickness. It was supposed that both the specific thermal capacity (Cp = 710 J/kg K) and the thermal conductivity (100 W/m/K) are constant and independent from the temperature. Graphite density of 2240 kg/m^3, reflectivity = 0,25 at 532 nm , and absorption coefficient of 1.5×10^7 m^{-1} were applied in numerical simulations. The results were obtained for the laser beam of 5 ns pulse duration and 0.7 J/cm^2 fluency. The conclusions were made that in order to reach the graphite evaporation temperature (4623 K) one should apply the laser fluency of 1.3 J/cm^2 that is comparable with the laser ablation threshold of graphite.

LASER ABLATION

With the laser radiation power increase, the temperature of a solid matter becomes higher than its melting temperature. The heated matter begins to evaporate intensively from the surface, that is, an ablation process is in progress. The laser ablation velocity during the thermal evaporation of the matter may be written as:

$$\upsilon(m/s) = \upsilon_0 \exp\left(-Ta/T(F)\right),$$

where υ_0 and T_a are constants. The laser ablation results in formation of a crater depth expressed as $h(F)=\int_0^\infty \upsilon(F,t)dt$, that is found to depend on the energy fluency F. For matters with high surface absorption (graphite, metals), the dependences h = f(F) may be characterized by three ranges [3] that correspond to the energy fluency: $F < F_{th}$, $F \sim F_{th}$, and $F = (2.5 \div 5)\, F_{th}$, where F_{th} – a threshold fluency.

With $F < F_{th}$, the crater depth that was formed during the laser pulse duration τ_L may be determined by $h = A\exp\left(Ta/Tmax\right)$, where $A \approx \sqrt{2\pi}\upsilon_0\tau L \left(Tmax/Ta\right)^{0.5}$ and T_{max} – the maximum temperature of the surface heating. With $F \sim F_{th}$, the thickness of the evaporated layer (the crater depth) is found to depend linearly on the energy fluency and is determined by the expression: $h = \beta(F - F_{th})$, where $\beta \approx (1-R)/L$, R – surface reflectivity coefficient, L – specific heat of evaporation for a solid matter. With a sufficiently high laser radiation fluency ($F > 2.5\ F_{th}$), plasma shielding is found to affect laser ablation. It was suggested to relate the crater depth to the radiation fluency by the expression: $F = B \exp(\alpha_g h) \ln^{-1}(A/h)$, where A and B – certain constants, α_g – efficient coefficient of laser absorption in plasma $F_a = F \exp(-\alpha_g h)$ normalized to the density of a solid matter. With a high radiation, when the radiation absorption in plasma is very significant, this expression takes the logarithmic form: $h = \alpha^{-1}{}_g \ln\left(F/F_g\right)$, where $Fg = B/\ln\left(\alpha g A\right)$.

Thus, depending on the laser fluency range, the crater depth increase takes the Arrenius form $h = A\times \exp(-B/F)$ for $F < F_{th}$. It is determined to be of the linear dependence from the laser fluency $h \sim F$ for $F \sim F_{th}$. It is of the logarithmic dependence from the laser fluency $h \sim \ln(F/F_g)$ for $F > 2.5F_{th}$. Given the experimental dependences of the crater depth from the laser fluency, it is possible to define the ablation regime from the dependence h = f (F) and to determine also the constants in the expressions for laser ablation. With these constants, it is possible to predict the crater depth values for any given laser fluency (F) affecting the solid matter.

CONCLUSIONS

It was found that a thermal model of laser heating and ablation of graphite co-deposited layer can be applied for an adequate description of surface detritation with cw- or high-repetition rate nanosecond lasers. The theoretical model should take into consideration both the real optical and thermo-physical properties of reactor graphite walls with a co-deposited layer. A co-deposited carbon layer can be characterized by the features (porosity, density, thermal conductivity, and so on) that are determined to differ significantly from the properties of graphite tile surface.

Laser heating and ablation simulation should take into account the variety of properties of a surface suffering the laser radiation. In this respect, our previous results on the simulation of laser heating may be regarded as valuable. The study was made on the laser heating of a metal surface with an oxide layer of 1–100 μm thickness [4]. Certain modifications of our model should be made to incorporate the specific features of a co-deposited graphite layer.

Thus, further theoretical and experimental studies on optimization of thermo-fusion reactor walls detritation by laser heating or by ablation of a co-deposited layer are required.

The experimental and theoretical studies on laser heating and ablation should be made simultaneously to improve the theoretical models and to verify them with the real structure and peculiarities of reactor surfaces.

In order to develop an adequate and verified theoretical model for laser detritation and ablation based on the graphite parameters, it is necessary to use the temperature-dependent thermo-physical properties of reactor graphite with co-deposited layer.

The improved model is expected to give an adequate description of laser heating and ablation for detritation and cleaning of the reactor chamber walls. An adequate simulation for laser heating and graphite ablation will allow to determine the most optimal regimes for detritation of reactor surfaces with a different degree of contamination.

REFERENCES

[1] Carslaw H.S., Jaeger J.C., "Conduction of Heat in Solids", Oxford Univ. Press, Oxford, 1959.

[2] C.H.Skinner, H. Kugel, D. Mueller, B.L.Doyle, W.R. Wampler, "Tritium Removal by CO_2 laser heating", Proceedings of SOFE'97, CH 36131 Vol. 1 (1998) 321.

[3] Anisimov S.I., Luk'yanchuk B.S., Physics-Uspekhi, vol. 45 (3), 2002, p. 293-324.

[4] Fomichev S.V., Semerok A., Report CEA, DPC/SCPA/NT02-053, 2002, 27 pages.

REPORTS AND PUBLICATIONS

Bibliography Study on Co-deposited Layer and Laser Detritation Processes - F. Le Guern, J.-M.Weulersse - Report CEA, NT DEN/DPC/SCP/LILM/2003-06, 2003, 13 pages.

Bibliography Study on Theoretical Models of Laser Detritation Processes - A. Semerok, J.-M. Weulersse - Report CEA, NT DEN/DPC/SCP 03-069-A, 2003, 28 pages.

TASK LEADERS

A. SEMEROK, JM. WEULERSSE, F. LE GUERN

DEN/DPC/SCP/LILM
CEA-Saclay
F-91191 Gif-sur-Yvette Cedex

Tél. : 33 1 69 08 65 57
Fax : 33 1 69 08 78 84

E-mail : asemerok@cea.fr

UT-S&E-LiPbwater

Task Title: MODELLING OF THE INTERACTION BETWEEN LITHIUM-LEAD AND WATER USING THE SIMMER-III CODE

INTRODUCTION

In the frame of safety studies on fusion reactor, the postulated interaction between lithium-lead alloy, used to produce tritium to maintain the fusion reaction, and cooling water could lead to a loss of integrity of the compartment in which it occurs.

Interaction tests between this liquid metal and water were carried out at Brasimone for this purpose on the LIFUS facility in order to understand the behaviour under different geometrical conditions and for different physical properties (temperature, pressure). The tests were modelled and analysed using the severe accident software SIMMER-III. The calculation results are in satisfactory agreement with the experimental data. Only the pressure level reached during the interaction is underestimated by SIMMER. The 2003 task was to review the possible causes of this difference and to present results of new investigations taking into account some improvements made for this purpose in the SIMMER modelling.

2003 ACTIVITIES

Before simulating the LIFUS test n°4, a brief recall of the experiment is presented. The test has consisted in ejecting pressurized water into the lithium-lead tank. At the contact of the two liquids, water is rapidly vaporised. Under this phenomenon, pressure increased sharply in the reaction vessel, ejecting the mixture of fluids through the expansion tube. Pressure was then stabilized for a while before hydrogen, generated during the interaction, led to a new increase of vessel pressure.

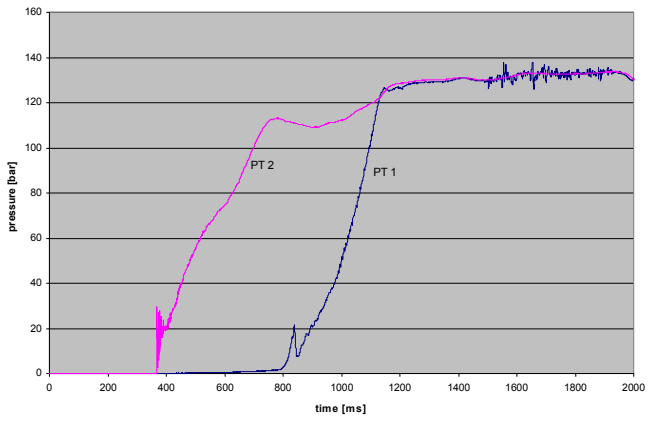

(PT2: interaction tank pressure, PT1 : expansion tank pressure)

Figure 1 : LIFUS test n°4, pressure evolution within interaction and expansion tanks

During the thermal interaction phase, the results of test n°4 show that:

- at the beginning of the injection of liquid water (around 380 ms), the pressure rapidly increases (increase rate of 260 bar/s) to reach a maximum value of roughly 113 bar at 775 ms,
- the pressure wave then decreases more slowly to a minimum value of 109 bar obtained at 900 ms,
- the pressure then increases again up to a value of 126 bar obtained at 1150 ms ; this pressure level is simultaneously reached in both tanks,
- in the rest of the transient, the pressure in both tanks is nearly identical and is maintained at 130 bar.

SIMMER RESULTS ON LIFUS TEST N°4

The phenomenology of the first part of interaction between the two fluids for test n°4 was well simulated by SIMMER-III. The comparison was detailed in a dedicated report [1]. A major difference in the comparison between experiment and calculation has been however highlighted. It concerns the pressure level reached during the interaction in the reaction vessel. The calculated underestimation of the pressure was interpreted as a wrong calculation of the water partial pressure.

Even though the pressure peak is underestimated, the results remain encouraging, especially on the evaluation of the delay in compressing the expansion tank. Associated to the verification of the basic hypothesis when changing to the Cartesian geometry, this calculation indirectly shows that the proportion of injected water mass in the interaction tank seems to be correctly reproduced. Nevertheless, some doubts on the heat transfer modeling between metal liquid and water were mentioned. Explanations for this difference were proposed [2].

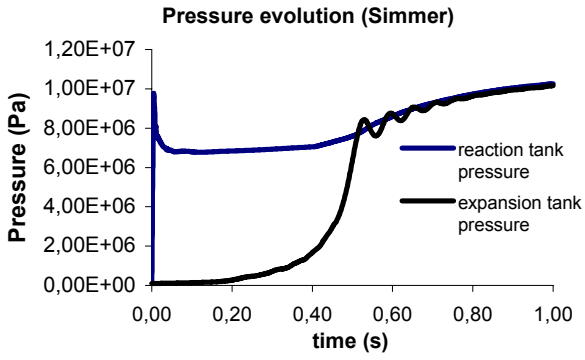

Figure 2 : SIMMER pressure evolution within interaction and expansion tanks

POSSIBLE EXPLANATION FOR PRESSURE UNDERESTIMATION

The presence of water under two phases was suspected to be responsible for the discrepancy between calculation and experiment in the pressure evaluation. Due to residual liquid water, partial pressure is calculated with SIMMER-III on the saturation curve, without taking into account the vapour characteristics.

Indeed, if liquid water is in small amount in a SIMMER mesh, which is consistent with the LIFUS calculation since water is vaporised at the contact of the lithium-lead alloy, liquid water does not participate to heat transfers. In this case, water temperature is set to the corresponding saturation temperature. Temperature evolution and partial pressure are therefore blocked. This behaviour could be probably the source of the underestimation on the interaction pressure.

Other points have been discussed which could explain the discrepancies between the experiment and the SIMMER-III code:

- water saturation pressure law by the code,
- abnormal value of the liquid water and pressure temperature in the interaction tank,
- pressurization of the system,
- overheated vapor state,
- basic hypotheses when changing to Cartesian representation,- mass of water injected,
- presence or absence of hydrogen during the thermal interaction phase.

PROPOSED SOLUTIONS TO IMPROVE THE EVALUATION OF THE PRESSURE

A SIMMER correction was made to vaporize the residual liquid water by liquid/liquid vaporization process.

This new option led to minor effect on the result. The difference in pressure reached in the interaction vessel is less than 1 bar during the test.

Due to the uncertainty on the injector modeling, it was suggested to modify the velocity of injected water.

Pressure was kept at 155 bar and an initial velocity of 1m/s instead of 0 was imposed to the liquid water. Pressures were highly lower than in the standard case. So, it was decided to keep their initial velocity to 0. This is a conservative approach, which also gives more realistic results.

A modification of boundary conditions near the injector, in order to take into account for the loss of pressure at the outlet of the injector, was also proposed.

The effect is negligible on the pressure variation in the expansion and reaction tanks.

In order to start water vaporization earlier, saturation temperature was decreased in the SIMMER modeling and imposed at 325°C instead of 345°C at 155 bar. No effects were also obtained on the results.

CONCLUSIONS

The purpose was to highlight and to explain the discrepancies in pressure evaluation made by SIMMER in the reaction vessel by doing some parametric studies and an improved modelling.

Modification of the liquid water effect is not sufficient to explain the difference in pressure. A better representation of the injector also has an impact on the results, as well as the choice of different boundary conditions. However, these modifications can only partially explain the difference between calculation and experiment. Future work is proposed, based on the real 3D modelling of the interaction vessel using the 3D version SIMMER-IV.

REPORTS AND PUBLICATIONS

[1] “Cartesian representation of LIFUS-5 with SIMMER-III code and application to test n°4” January 2003. CEA Report by P. Sardain, T. Jeanne.

[2] “Modelling of the interaction between lithium-lead and water using the SIMMER-III code” January 2004. CEA Report by Thierry CADIOU.

TASK LEADER

Thierry CADIOU

DEN/DER/SESI/LCSI
CEA-Cadarache
F-13108 Saint Paul Lez Durance Cedex

Tél. : 33 4 42 25 66 17
Fax : 33 4 42 25 71 87

E-mail : cadiou@monet.cad.cea.fr